INTERFACE SCIENCE 9, 117–129, 2001

Dynamics of Ice Surfaces

J.S. WETTLAUFER
Applied Physics Laboratory and Department of Physics, University of Washington, Seattle, WA 98105-5640

Abstract. The dynamics of faceted and partially faceted single crystal and polycrystalline ice are reviewed with an emphasis on the manner in which microscopic effects produce macroscopic shapes. Our understanding of the former is rooted in the basic kinetics common to all materials and our pursuit of the latter is largely motivated by the striking patterns exhibited in the natural environment when water changes phase to become ice.

Keywords: ice, surface melting, roughening transition, kinetics, anisotropy, grain boundary

I. Introduction

The most striking feature of crystalline material is its shape. As experts and laymen alike we often fail to appreciate that in admiring the form of a stone or a snowflake, what we see is typically not an equilibrium shape, but rather, the result of a growth process and subsequent isolation from efficient kinetic pathways that allow the material to equilibrate. Historically, our understanding of the relation between growth and equilibrium shapes emerges out of the aesthetics of geometry *and* the desire to control matter. However, in the study of ice many of the observed patterns arise out of the uncontrollable influence that the natural environment renders on growth forms.

Ice dominates the crystal growth phenomena we observe on the surface of the earth and in the atmosphere. The surface-specific structural phase transitions known as interfacial melting, and surface and kinetic roughening are observed to occur in ice, and as in other materials, such factors influence equilibrium and growth forms. However, as opposed to many technological materials, ice exists in the terrestrial environment at temperatures relatively close to its melting point. Through their influence on the interfacial structure, these surface phase transitions can control the adsorption potential, the growth shapes and surface transport properties of ice. Moreover, because surface phase transitions occur in most materials, what we learn in ice is broadly relevant in condensed matter science.

During the winter of 1635 Descartes made strikingly detailed observations of snow and ice that, among other things, highlight the role of ice surfaces in growth, melting and adhesive behavior. Some of these observations were translated from French by Sir Charles Frank [1];

> *"The following morning, there fell flocks of snow, which seemed to be composed of an infinite number of little stars joined together; however, inspecting them more closely, I found that those in the interior were less regularly shaped than those at the surface..."*
> *"I was not surprised, either, to see often two stars of unequal size joined together...I judged that the cause was that the heat, having been stronger around the small one than the other, had to a greater extent melted and blunted its points."*

Some two centuries later, in a series of investigations in which he questioned the role of the surface in the slipperiness of ice, Michael Faraday initiated thoughts on what we now refer to as surface melting [2]. Modern research into the mechanisms underlying pattern formation in snowflakes is traced to the experiments of Nakaya [3, 4] in which the first systematic laboratory studies correlated growth conditions with crystal shapes. Today we continue to explore and unravel the mysteries exposed by Descartes.

II. Equilibrium Phenomena

A. Equilibrium Crystal Shapes

The earliest research efforts to understand the shapes of growing crystals underlie our understanding of their equilibrium forms. Wulff [5] developed the concepts of global geometry arising from an extremum principle wherein the total surface free energy of a crystal at fixed volume is minimized. Experiments, exact solutions of microscopic models, and meanfield theory have demonstrated that an ideal, dislocation free, equilibrium shape of a crystal depends on temperature: It is fully faceted at absolute zero, and becomes more rounded, or locally rough, as its temperature increases (reviews can be found in refs. [6, 7], and [8]). When the dominant intermolecular interactions in the material are short ranged, the bond energies can be estimated by considering only nearest neighbors in the lattice. In this manner we can build a picture of the surface free energy of a crystal, $\gamma(\hat{\mathbf{n}})$, as the sum of the energies of all the bonds broken per unit area in the creation of the surface of an orientation $\hat{\mathbf{n}}$ relative to the underlying crystalline lattice. Were we in possession of the surface free energy of the crystal as a function of all orientations present, the geometric Wulff construction will determine the equilibrium crystal shape (e.g., [5, 9, 10]). Conversely however, were one to measure the shape of a crystal in equilibrium, the Wulff construction will provide the surface free energy for all orientations present on that shape (e.g., [11]). Because of the long equilibration times, observations of true equilibrium forms are rare, but ice in contact with the melt phase (Fig. 1) and negative crystals of ice are reasonably practicable to produce and offer excellent forms for theoretical tests [12, 13].

B. Surface Roughening

As described above, structural surface phase transitions are of broad importance in natural and technological settings. We characterize a surface by the free energy of the various interfacial configurations: faces, ledges, corners, edges, and point-defects such as admolecules and vacancies. The energy cost associated with any state is the sum of the formation enthalpies of the sites, and this is weighed against the lowering of the total free energy derived from increasing the configurational entropy of the surface—the driving force for the thermodynamic roughening transition. As the temperature rises, thermal fluctuations continually produce steps. Forming a regular array of steps is tantamount to slightly tilting the surface, which requires doing some work against the periodic potential of the underlying crystalline array. The coherence length of the surface, $\eta(T)$, is a measure of the distance, relative to the mean orientation of the surface, over which fluctuations at two points are correlated (e.g., [7]). As the temperature T increases, the free energy cost of a step, $\sigma_s(T)$, decreases. For an infinite two-dimensional surface $\sigma_s(T) \rightarrow 0$ at the roughening temperature, T_r, and therefore the coherence length, $\eta(T) = \gamma(\hat{\mathbf{n}})/\sigma_s(T)$ diverges. Hence, thermal agitation liberates the surface from the ordering influence of the underlying crystalline lattice and fluctuations are correlated on all length scales so that the surface roughens.

Facets in real crystals are of course finite. As the temperature rises and the step free energy falls, $\eta(T)$ approaches the facet size, and facets roughen at $T = T_f < T_r$. If $T > T_f$ for all facets present, an equilibrium shape will be completely rough and rounded. Because of the importance of these effects in electronic materials, there is a large literature (see e.g., [14]), and although theoretical treatments are in qualitative agreement, predictions of T_r and T_f are strongly model dependent. Clearly because it is responsible for a substantial interfacial restructuring, the roughening transition profoundly influences the dynamics of molecules on the surface. An important consequence of this concerns nonequilibrium phenomenon that cause a related transition known as the kinetic or dynamic roughening transition, which occurs when the growth rate exceeds a critical value [15]. There are other distinct, but closely related transitions associated with surface reconstruction that have not been observed in ice, but which are fundamentally important and often observed in other materials [16].

The roughening transition of the prism facet of ice I_h has been observed under vapor conditions by Elbaum [17]. Maruyama performed a series of experiments over a tremendous thermodynamic range for ice in contact with water [18]. He observed both the roughening transition of the prism facet of ice I_h and the changes of the equilibrium crystal shape by carefully controlling the pressure, at fixed temperature, along the solid-liquid coexistence line from near the triple point to -21°C at 200 MPa. What he found was that prism facets undergo a thermodynamic roughening transition at approximately -16°C at 165 MPa. The technique has the ability to accurately control the growth drive very near

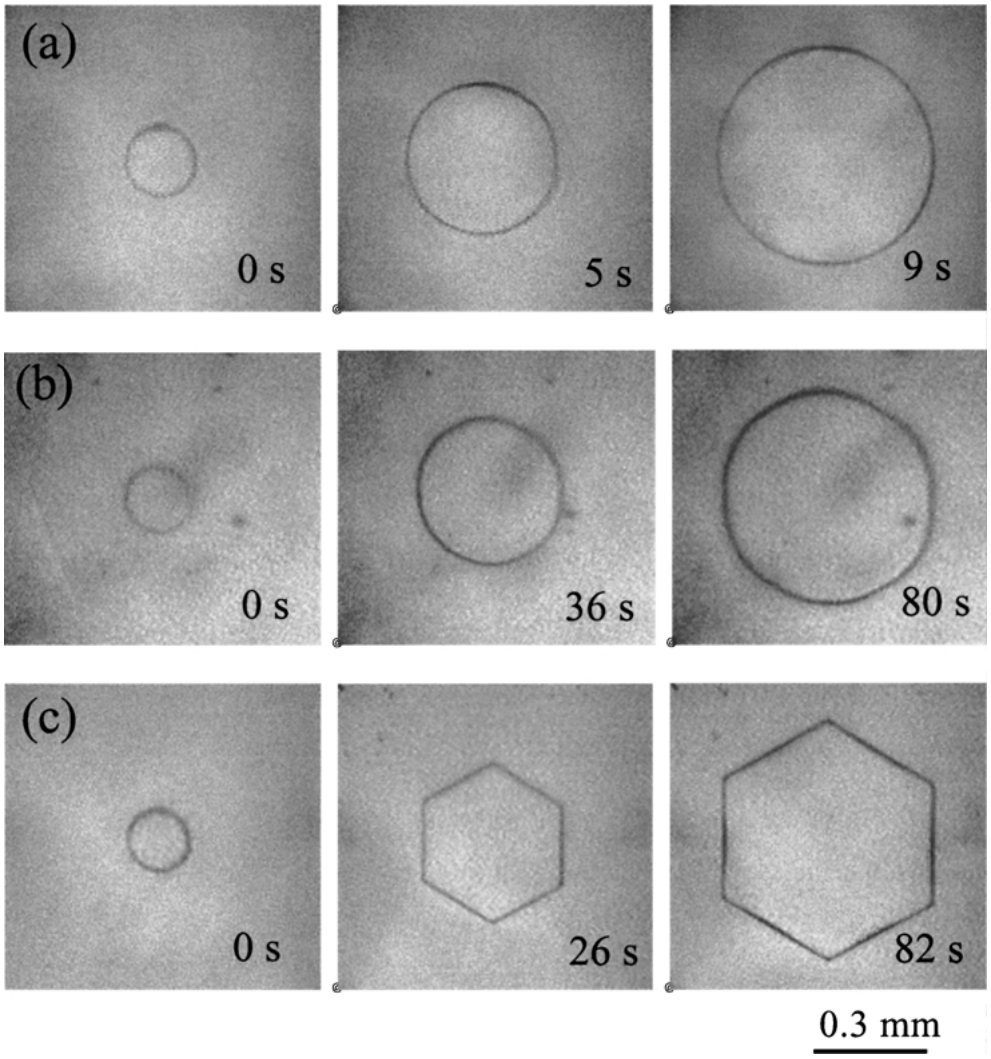

Figure 1. Growth sequences of ice above, just above and below the roughening temperature of the prism facet which is -16°C. Water is contained in a Bridgman apparatus and held at fixed temperature while pressure is used to control growth which is observed parallel to the c-axis using an optical microscope as described in refs. [18, 51]. By this method a crystal can be "walked" along solid-liquid coexistence and small growth drives can be imposed. The equilibrium temperature and pressure are measured at 0 seconds. The normalized growth drive, $\Delta\mu/kT$, is applied after zero seconds. (a) $T = -5.68^{\circ}$C, $P = 666$ bars, $\Delta\mu/kT = 3.3 \times 10^{-4}$ (b) $T = -14.45^{\circ}$C, $P = 1513$ bars, $\Delta\mu/kT = 3.5 \times 10^{-4}$ (c) $T = -20.24^{\circ}$C, $P = 2029$ bars, $\Delta\mu/kT = 4.0 \times 10^{-4}$. Data kindly provided by Y. Kishimoto and M. Maruyama.

equilibrium and hence can test theoretical predictions of crystal shapes growing and melting near equilibrium, which is described below.

C. *Surface Melting*

Equilibrium forms are necessary to study equilibrium surface phase transitions. At temperatures far below the bulk melting transition, T_m, the free surfaces of most materials possess a structure that is largely reflective of the long-range periodic order of the underlying lattice. However, because of the missing bonds at the surface, as the temperature rises the outermost molecules experience a greater anharmonicity in their vibrations. This causes the outer layers to disorder more readily as the temperature rises toward the bulk melting point. Typically, as the temperature approaches 0.9 T_m the surface adopts a liquid like structure; *surface melting*. The melt has some attributes of the solid below and some of the bulk liquid, and as the temperature continues to rise

toward bulk coexistence the film thickness d diverges. Surface melting has been observed on at least one crystallographic facet in virtually all materials, including metals, semiconductors, rare gas and organic solids, and ice [19–23]. The equilibrium thickness of the melt layer depends on the temperature and the molecular interactions between the components of the system.

For materials controlled by dispersion forces, the thickness d is given by

$$d = \left(- \frac{2\bar{\sigma}^2 \Delta\gamma}{\rho_\ell q_m t} \right)^{1/3}, \tag{1}$$

where q_m is the latent heat of fusion, $\bar{\sigma}$ is a length on the order of a molecular distance, ρ_ℓ is the molecular density of the liquid, $t = (T_m - T)/T_m$ is the reduced temperature, and $\Delta\gamma$ is the difference in interfacial free energies between the dry and surface melted states. When the surface interactions are short ranged, the thickness relation is logarithmic:

$$d = d_o \ell n \left(- \frac{a_o \Delta\gamma}{\rho_\ell q_m t} \right) \tag{2}$$

where d_o and a_o are constants (see e.g., [22]). Other interactions, such as electrostatic forces, can produce other similarly specific temperature dependences [24].

Early tests of the theory of surface melting were made in metals [21], wherein the dominant interactions are short ranged, and rare gas solids, in which dispersion forces dominate [25]. For example, in Ar and Ne, surface melting of the outermost layers begins above about 0.8 T_m, and the rate of increase of the liquid thickness with temperature is slow until very close to the transition [25].

Surface and interfacial melting are enhanced by nonequilibrium disorder in the neighborhood of the solid surface, by raising the local free energy of the solid relative to that of the liquid. Several possible forms of disorder can produce such an effect: roughness, polycrystallinity, strains and dislocations, and the presence of impurities [26–29]. Recently, a state theory of damage assisted interfacial melting has been developed to explain collisional charging in ice [30].

Although they clearly show the effect, laboratory experiments on the surface melting of ice are extremely variable quantitatively. This variability lies in both the great sensitivity to the atmosphere and conditions of preparation [29], and in the inherent differences in measurement technique; proton backscattering [31], ellipsometry [32, 33], optical reflectometry and interference microscopy [34], X-ray diffraction [35], glancing angle X-ray scattering [36], and sum-frequency vibrational spectroscopy [37]. These methods are designed to measure different structural aspects of the surface and hence there is still active debate in the community regarding the intepretation of the various results throughout the entire temperature range [38, 39]. Despite this variability, what we can say with certainty is that sufficiently close to the bulk melting transition, the growth kinetics at the vapor or gaseous atmosphere surface of ice will be altered [12, 40–42], but quantitative explanation of these issues is an area of future exploration.

III. Nonequilibrium Phenomena

A. Growth of Partially Faceted Single Crystals

A principal curiosity of crystal growth is that it provides a setting in which microscopic phenomena control macroscopic shapes. Advances in our understanding help inform many areas of science and technology, from atmospheric science and computer chip manufacturing to powder metallurgy. Moreover, because growth shapes are often cast in the form of a free boundary problem, there are a myriad of theoretical analogues in hydrodynamic, chemical and biological systems (e.g., [43–45]).

In a laboratory system, crystal growth very close to equilibrium can be achieved (e.g., [11, 18, 34, 46]). However, when the growth drive is removed, a crystal growth shape must eventually relax to the equilibrium form, and the relaxation time depends on the mechanism facilitating the redistribution of material. For example, when surface diffusion dominates the relaxation times are typically extremely long [47]. Many of the crystals that we find in the natural environment and in metallurgical settings evolve from the melt phase and involve length scales that span many orders of magnitude. Curiously however, there are very few quantitative tests of theories. The growth of all crystals typically involves at least one principal facet, and ice is certainly no exception. As mentioned above, qualitative understanding of the dynamics of partially faceted crystals originates in the work of Wulff [5], Frank [48] and Chernov [49]. Because the accretion of material normal to facets is an activated process whereas no nucleation barrier exists for rough orientations, partially faceted equilibrium shapes become

more faceted during growth (e.g., see [50]). Therefore, for a spatially uniform growth drive, the rough orientations grow more rapidly leaving facets to dominate the shape. These qualitative features are known, but the general mechanisms underlying the process have remained as issue of research. Here I review our recent tests of such processes [51].

Typical models in which the local normal motion is maximal at locations wherein the step density is the highest predict that the rough orientations grow out of existence with *increasing curvature*. In contrast, models including effects such as surface diffusion, find that the growth rate may not be a maximum where the step density is the highest. This leads to the prediction that the loss of rough orientations occurs via a local *decrease* in curvature, which results in the formation of discontinuities, or shocks, in the surface of the growth forms. Because the evolution of a given orientation depends on the microscopic details influencing the attachment of additional molecules, tests of such theories on macroscopic shapes provide unique probes of microscopic kinetics.

Theories must reconcile the coexistence of faceted and rough interfacial states on a single closed surface. In situations in which the motion of the interface is limited by local interfacial processes, we can treat it as *geometric* in the sense that the normal velocity at an interfacial point depends on the *shape* and *position* of the interface, and not on field variables modified by the interface motion or long-range diffusion in the bulk (see e.g., [52]). Such models are broadly useful in natural and laboratory systems, for example, the early stages of snowflake growth, when the mean free path in the vapor is larger than the characteristic size of the crystal, the growth of materials via molecular beam epitaxy, among others.

It is useful to distinguish the principal limits in terms of the magnitude of the growth drive $\Delta\mu$, the chemical potential difference between a molecule in the parent phase and that on the solid. We begin at extremely small $\Delta\mu$, wherein the accretion of mass is much slower than all of the available relaxation processes, so that the crystal surface is indistinguishable from the equilibrium crystal shape. This "thermodynamically slow" or "shape preserving" regime has been observed at temperatures above, below and very near the roughening transition of the prism facet of ice growing from water (see Fig. 1), and can be described via a continuous expansion of the Wulff shape [53]. As $\Delta\mu$ becomes larger, but nonetheless smaller than the activation barrier for nucleation on the facets $\Delta\mu^*$, the facets remain pinned and the rough orientations accrete mass to take the Wulff shape of an "equilibrium" crystal of increasing size [53, 54]. Ultimately the rough orientations grow themselves out of existence leaving a fully faceted growth form behind. If we further increase $\Delta\mu$ to a value that is above $\Delta\mu^*$ but below the threshold necessary to induce kinetic roughening on the facets, $\Delta\mu_{kr}$, the facets grow slowly by nucleation and spreading of monolayers.

We have focused on two dimensions which is more than just a mathematical convenience, for it is relevant to the growth of nuclei on a facet [55, 56], the growth of highly anisotropic materials such as ice [57, 58], the evolution of monolayer surfactant films [59, 60], or the growth of axisymmetric three-dimensional crystals as described presently. A geometric model has been constructed around an equation for the local normal velocity, $V(\theta, \Delta\mu)$ that explicitly accounts for activated growth on facets, nonactivated growth in rough regions and their modification in the vicinal orientations in a continuous manner [54]. $V(\theta, \Delta\mu)$ depends on a spatially uniform driving force, $\Delta\mu$, and the orientation of the surface with respect to the underlying lattice θ as follows;

$$V(\theta, \Delta\mu) = V_f(\Delta\mu)\xi(\theta) + V_g(\theta, \Delta\mu)(1 - \xi(\theta)), \tag{3}$$

where V_f and V_g are the growth laws on facets and rough orientations, respectively, and take the form $V_f(\Delta\mu) = f(\Delta\mu)\exp(\frac{-\pi\sigma^2}{kT\Delta\mu})$, and $V_g(\theta, \Delta\mu) = g\Delta\mu[1 + \cos^p(\frac{n\theta}{2})]$. The free energy of a critical nucleus on the facet is denoted σ, and $\xi(\theta) = \cos^m(\frac{n\theta}{2})$ determines the nature of the transition between facet-like and rough growth.[1] The mobility coefficients f, g are influenced by the molecular attachment kinetics, and the growth rate in vicinal regions has contributions from both the birth and spreading of supercritical islands on terraces *and* molecular attachment directly to kinks in moving steps. The combined influence of these two effects on the normal growth rate is embodied in the second term of $V_g(\theta, \Delta\mu)$. An essential qualitative point is that, for a given $\Delta\mu$, $V_f \ll V_g$. This description is valid for n-fold symmetry, and m and p are even integers such that $m \geq p$. The function described by Eq. (3) is the simplest form capturing growth anisotropy in the continuum limit. Other geometric growth models (e.g., [52, 61]) represent anisotropy as a product of an orientation dependent mobility and a linear combination

of a bulk phase change contribution and weighted mean curvature, itself a linear combination of $\gamma(\hat{\mathbf{n}})$ and $d^2\gamma(\hat{\mathbf{n}})/d\theta^2$. We view the anisotropy in the kinetics as arising out of that in the surface energy, which is not strictly defined away from equilibrium, and hence our model is based on the statistical mechanics of the surface, but it is essentially kinematic.

By suitable application of the differential geometry of curves in the plane [e.g., 54, 56, 57, 62] the evolution of the curvature κ of the surface can be written as

$$\frac{\partial \kappa}{\partial \tau} = -\kappa^2 \tilde{V}, \tag{4}$$

in which $\tilde{V} \equiv (V + \frac{\partial^2 V}{\partial \theta^2})$ is the "velocity stiffness" in *analogy* with the surface stiffness of the equilibrium shape [9], and $\frac{\partial}{\partial \tau}$ is a time derivative taken at constant θ. The curvature evolution at each point of the interface with initial curvature κ_i then follows immediately as,

$$\kappa = \frac{\kappa_i}{1 + \kappa_i \tilde{V} \tau}. \tag{5}$$

In the simplest general case of cubic symmetry ($n = 4$) and $m = p = 2$, or $m = 4$ and $p = 2$, we find that $\tilde{V} > 0$ for orientations between the facets, and hence it is predicted that the curvature will *decrease* monotonically in time from the initial value at that orientation. We can understand this decrease as being due to a tendency toward a constant surface density of steps; in vicinal regions surface diffusion on the terraces enhances motion normal to the interface, increases the density of sites for attachment and drives the region toward a more constant step density. The effect can be described as a kind of "dynamical faceting". In contrast, models in which regions with the highest surface density of steps grow the fastest may have $\tilde{V} < 0$ and this is inconsistent with experiment as shown below.

Although ice is the material that captures our principal efforts, controlled growth from the melt phase with optical resolution sufficient to test theory is notoriously difficult [18]. However, given the generality of the theory described above, what we find for another material is relevant to ice upon suitable symmetry transformations. In this vein, we have examined a fourfold symmetric crystal as an experimental system; carbon tetrachloride (CCl_4) grown from the melt under pressure. Owing to a rhombohedral unit cell with 90° in the lattice angle [63], CCl_4 grows in a cubic form [64]. Moreover, growth from the melt at fixed temperature and at moderately high pressures (<1000 bar) has enabled us to accurately control parameters such as initial curvature and growth drive [51]. Pressure transmits to the sample quickly and uniformly under hydrostatic conditions. Hence, through simultaneous pressure manipulation and visual inspection, we can produce a partially faceted crystal and then grow it at very small growth drives thereby providing an ideal test of geometric models.

The experimental procedure is as follows. At a constant temperature of 5°C, liquid CCl_4 sealed in an elastic fluorocarbon tube is pressurized by manual operation of a hand pump. Spontaneous solidification into a polycrystalline solid occurs at approximately 1000 bar. A single crystal is then obtained by reducing the pressure below an equilibrium value (∼750 bar) and melting the polycrystal until only one crystallite remains. A cubic crystal can be made with continuous curvature between the facets and subsequently grown. Upon imposition of a small growth drive to such a partially faceted crystal, we observe the essential tenets of the theory of global kinetic faceting (see Fig. 2). The first feature of the theory that is observed is that discontinuities in the surface slope form abruptly, thereby separating rough orientations from vicinal and faceted orientations. These discontinuities are associated with the formation of shocks in the global curve dynamics [54]. The second feature we observe is that the rough regions grow out of existence with a *decreasing* curvature; the facets are not mobile and eventually dominate the overall shape. Neither of these features are predicted by models in which regions of high local curvature, where the surface density of steps is highest, grow the fastest [51, 54].

We have tested the theory quantitatively by measuring the relation between V and $\Delta\mu$ for facets and rough orientations (at $\theta = \pi/4$), and this is shown in Fig. 3. The rough orientations do indeed grow linearly with $\Delta\mu$, whereas activated growth is observed on facets. Due to the rapidity with which the rough orientations grow out of existence, observations of curvature evolution can only be made at the smallest growth drives. The radius of curvature of the curved surface between the facets is measured directly as a function of time and plotted in Fig. 4. The curvature is averaged about the $\theta = \pi/4$ orientation and has an accuracy of approximately 10%. It is observed that the curvature *decreases* linearly with time and the rate at which it does so increases with the growth drive as predicted by Eq. (5). Therefore we find that $\tilde{V} > 0$ at $\theta = \pi/4$, and we can estimate its value under the assumption

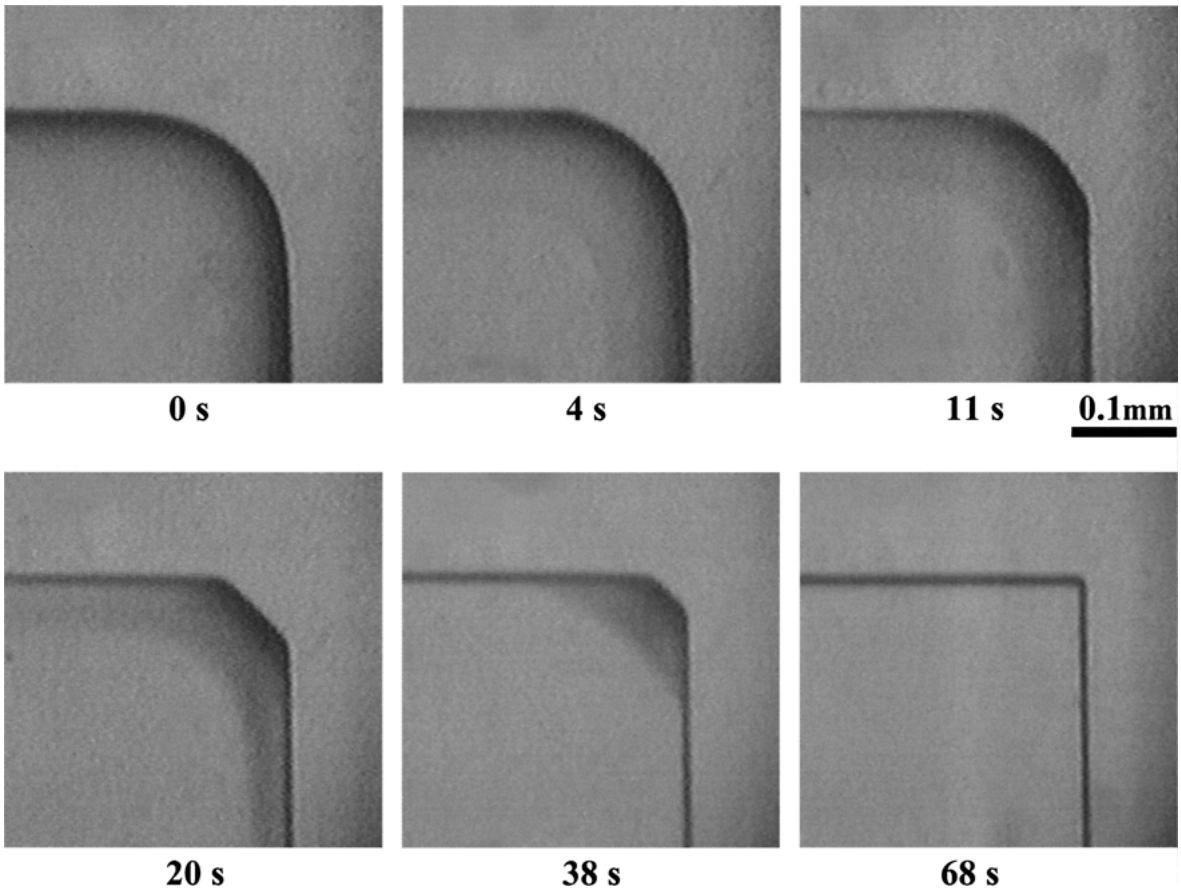

Figure 2. Growth sequence of a CCl_4 crystal in a high pressure melt. The initial shape contains facets and rough regions and we display the upper right hand quadrant of a cubic crystal. The growth drive (pressure deviation $\Delta P = 1$ bar) is applied at 0 s when the shape is equilibrated at $T = 5.33^{\circ}$C and $P_m = 754$ bar; $\Delta\mu$ is proportional to ΔP and $\Delta P = 1$ bar corresponds to $\Delta\mu/kT = 1.4 \times 10^{-4}$ [51]. Note (i) Discontinuities in the surface slope form abruptly after 4 s, and are more pronounced at 11 s, thereby separating rough orientations from vicinal and faceted orientations. Such discontinuities are associated with the formation of shocks in the global curve dynamics [54]. (ii) The rough orientations grow out of existence with *decreasing* curvature, while facets do not grow at all. The three-dimensional features are clearer at later stages. Adapted from [51].

that $\tilde{V}$ is the same order of magnitude as $V(\approx 1\ \mu$m/s). For experimental values of $\kappa_i \approx 10^4$ m^{-1} and $\tau \approx 20$ s, $\kappa_i \tilde{V} \tau \approx 0.2$ thereby yielding the relation $\kappa \approx \kappa_i - \kappa_i^2 \tilde{V} \tau$ from Eq. (3). These fits for rate of curvature decrease $\kappa_i^2 \tilde{V}$, as displayed in Fig. 2, give the following estimates: $\tilde{V} = 3 - 4\ \mu$m/s at $\Delta\mu/kT = 1.4 \times 10^{-4}$ and $\tilde{V} = 5 - 9\ \mu$/s at $\Delta\mu/kT = 2.8 \times 10^{-4}$.

A further curiosity that presently holds our attention is an apparent paradox between two implications of the same underlying geometric theory. On one hand, a cartesian description of the shape evolution leads to the prediction that the loss of rough orientations occurs via the formation of discontinuities, or shocks, in the surface. In such a surface, the curvature is bounded on either side of the shock. On the other hand, the description of the surface via its curvature (Eq. 5) predicts a finite time curvature divergence, which is a continuous process. The paradox is resolved in this class of models by the fact that the shocks form prior to continuous divergence of curvature. Previously we had obtained numerical evidence for this behavior [54], and recently we have been able to provide mathematical proof for it [66].

These observations display the general macroscopic influence of anisotropy in microscopic crystal growth kinetics: the relaxation rate at rough orientations is negligible compared with that on the facets, and hence the latter spread to dominate the growth form.

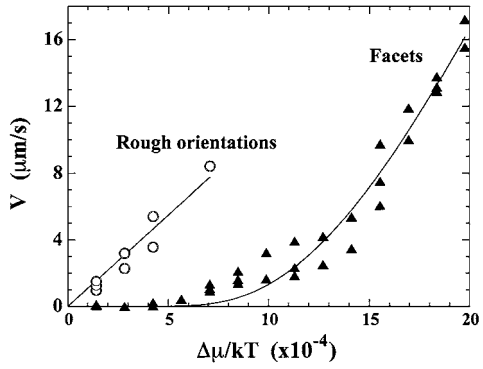

Figure 3. V versus $\Delta\mu/kT$ for rough orientations at $\theta = \pi/4$ and facets. Fits are linear and exponential, respectively. For rough orientations V can not be measured at larger $\Delta\mu$ due to rapid faceting. Adapted from [51].

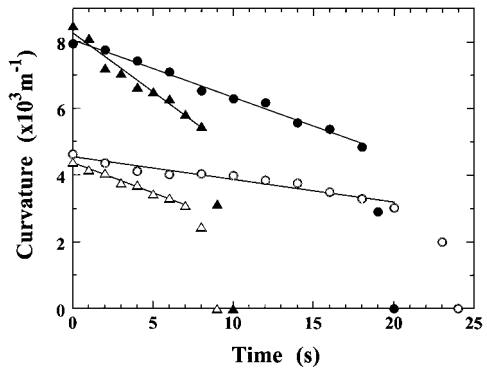

Figure 4. Curvature evolution and fits for $\tilde{V}$ at two initial curvatures and two growth drives. Solid symbols are at $\kappa_i \approx 8 \times 10^3$ m^{-1}, $T = 5.33^\circ$C and $P_m = 754$ bar; open symbols are at $\kappa_i \approx 4 \times 10^3$ m^{-1}, $T = 5.08^\circ$C and $P_m = 749$ bar. Circles are at $\Delta\mu/kT = 1.4|, \times 10^{-4} (\Delta P = 1$ bar); triangles are at $\Delta\mu/kT = 2.8 \times 10^{-4}$ ($\Delta P = 2$ bar). Because the region of rough orientation between the discontinuities must shrink during the faceting process, the curvature eventually changes abruptly and the effects of dimensionality become important. Adapted from [51].

Such features are operative in all weakly driven partially faceted crystals. With the exception of very late times during the evolution, when the influence of faceting and dimensionality become important, the principal features of the two-dimensional theory are valid. The importance of such a study is that it forces us to examine the underlying assumptions of commonly accepted models and provides a framework for broad based testing of the kinetics of crystal growth in two and three dimensions. Moreover, it gives us confidence in our understanding of kinetics and their relevance to more complicated geometries as for example seen in the dynamics of partially faceted polycrystals.

B. Grain Boundary Dynamics

In our description of the growth of single crystals, we have focused on situations in which anisotropy controls the overall convex morphology. Although concavities are not present on an equilibrium shape, because they increase the chemical potential of the material relative to that of the bulk, they may arise from growth instabilities, wherein two regions of a surface advance at a rate that is greater than a region between them. The concavity may persist and thereby characterize the growth form; a common example is that of the snowflake. However, as we will discuss in this section, concavity arises naturally when two or more single crystals grow together.

An in important aspect of polycrystallinity in materials science centers around the influence that grain boundaries have on sample properties, whereas in the context of natural solidification from the melt, rarely does one find single crystals. When we bring a bicrystal in contact with its melt liquid the interface is indented by grooves where the two grains meet the liquid. In equilibrium, the depth and shape of a groove are determined by the relations between the three interfacial coefficients, but this shape is modified by the imposition of a temperature gradient [67, 68], an effect which forms the basis for a technique of measuring the solid-liquid interfacial energy [69, 70]. One typically finds grooves with smoothly rounded sides emerging from sharp clefts, although anisotropy of the crystal-melt surface energy can give rise to abrupt changes of slope [71]. In what follows I describe aspects of an interesting, although extreme, case of fully faceted grain boundary grooves that are observed in ice-water interfaces [72, 73]. Here again we find macroscopic consequences of microscopic processes wherein the rates of nucleation and spreading of elementary layers of the crystal are reflected in changes of the shape and size of the grooves.

As described in the previous section, the growth of singular surfaces is an activated process. The original theory assumed that nucleation is necessary only for sharp interfaces, and that rough interfaces could grow in the normal direction without supercooling [74]. Such theories can be modified to treat faceted grain boundary grooves, and allow one to show how the shape and size

of the grooves are systematically related to the rate of nucleation and spreading of individual layers.

1. Classical Grain Boundary Grooves. It is common to treat grain boundary grooves at a solid-melt interface in a manner analogous to the meniscus of a liquid that wets the wall of a vessel. The rise of the liquid meniscus, which replaces a dry interface by a wet one, is caused by the tendency to reduce the interfacial energy against the opposition of gravitational potential energy. At a solid-melt interface, a groove is caused by the difference between the solid-liquid interfacial energy and the grain boundary energy between the two crystallites, $\Delta\gamma$. Instead of gravitational energy, the depth is opposed by the free energy difference between the crystal and the supercooled liquid within the groove. Typical grooves are rounded faces and have a depth $\mathcal{L}$ given by

$$\mathcal{L} = \sqrt{\frac{\Delta\gamma T_m}{q_m \nabla T}}, \tag{6}$$

where ∇T is the temperature gradient within the liquid filling the groove. By studying grain boundary grooves in this manner it is possible to determine the interfacial energy of the ice-water interface [70]. We have studied grain boundary grooves at an ice-water interface in a thermally two-dimensional geometry [72, 73], and although it was found that most of the grooves were of typical rounded shape, and had depths consistent with estimates based on Eq. (6), a fraction were much deeper, with faceted sides, such as illustrated in Fig. 5.

2. Faceted Grooves and Their Dynamics. When orientations of singular crystal surfaces are tangent to the curved faces of a normal grain boundary groove faceted grooves can appear at a solid-liquid interface.

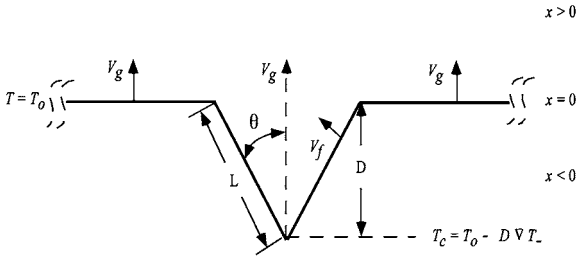

Figure 5. Schematic of a faceted grain boundary groove. Adapted from [73].

It is observed that in such a groove the singular facets can elongate continuously with temperature parallel to the surface, but they cannot advance in the direction normal to the surface until a portion of their surface is supercooled to the nucleation temperature. Upon application of a temperature gradient, the overall (bulk) interface advances, but the groove itself will deepen because normal growth is pinned until the groove depth is sufficient to lower the cleft temperature to the critical value. After this occurs new monolayers are nucleated at the cleft, where the temperature is lowest and where the grain boundary makes contact with the edge of the facet. At low freezing rates each layer can spread completely across the groove before the next layer is nucleated, so that the surface contains only one incomplete layer. As the solidification rate rises, the surface consists of several steps, and hence it is not perfectly parallel to a principal direction. The groove shape evolves smoothly, from fully single-faceted sides, to a combination of shorter facets and curved sections.

Here I outline our analysis of the growth dynamics in terms of the model illustrated in Fig. 5 and described in [73]. With the exception of the groove, ice fills the half space at $x < 0$, while water extends through $x > 0$. Because the bulk interface flanking the groove is above the roughening transition, in a steady state that part of the boundary, which is at $T = T_m$, proceeds at constant speed V_g in the $+x$ direction, under the impetus of the uniform temperature gradients ∇T_- $(x < 0)$ and ∇T_+ $(x > 0)$. The shape of the groove assumes that the time τ_p for a layer to spread parallel to its surface is short compared to the average time τ_n to nucleate a new layer, and hence each step crosses the surface completely before the next layer is nucleated.

In this regime, the faceted groove translates with the advancing interface by the nucleation of the layers on both sides near the cleft. Therefore, the nucleation time, the speed V_g of the bulk interface, the growth rate normal to the facet V_f, and the thickness of an elementary layer h are all related by:

$$V_g \sin\Theta = V_f = h/\tau_n, \tag{7}$$

where Θ is the inclination of the facet with respect to the x direction.

In accordance with classical nucleation theory [15, 75, 76] the nucleation rate $J = 1/\tau_n$ is an activated process from which we derived the growth rate at singular orientations V_f in terms of the growth drive $\Delta\mu$. The nucleation rate therefore depends on the free energy (line tension) of a critical nucleus on the facet σ

and the critical growth drive $\Delta\mu^* = \frac{\pi\sigma^2 T}{nq_m(T_m - T_c)}$ as

$$J = A(\Delta\mu)\exp\left(\frac{-\Delta\mu^*}{kT}\right), \tag{8}$$

where n is the two-dimensional density, and T_c is the temperature at the cleft, and the prefactor A is the initial growth rate of a critical nucleus. Note that in the general theory of nucleation, the prefactor is a quantity of considerable difficulty to measure and to describe theoretically even when invoking rather gross assumptions. For example, experiments with dislocation free Ga crystals indicate that $A \propto (T_m - T_c)^M$, where M depends on the facet [77], whereas Hillig [75] finds little evidence for such a dependence on basal plane facets of ice. For the present development we treat it as a constant, but we note that the same effect arises in the dynamics of partially faceted single crystals described above.

In the regime treated, we ignore the curvature of the isotherms within the cleft and assume a constant linear temperature gradient along the facet, $T(z) = T_m - Gz$, where the z coordinate is parallel to the facet plane with the origin located where the facet intersects the bulk interface at T_m and $G = (\nabla T_-)\cos\Theta$. The maximum undercooling is at the cleft, where $T = T_c$. As opposed to an isothermal facet, here the nucleation frequency J of two-dimensional islands of monomolecular height varies with temperature and hence position along the facet. Therefore, the probability of nucleation p varies with space as

$$p(z) = A\exp\left(\frac{-\pi\sigma^2}{knq_m[T_m - T(z)]}\right), \tag{9}$$

and hence in the faceted grain boundary groove, V_f depends on the length averaged probability distribution along the facet,

$$\begin{aligned} V_f &= \frac{A}{L}\int_0^L \exp\left(-\frac{c}{z}\right)dz \\ &= hA\left[\exp\left(-\frac{c}{L}\right) - E\left(\frac{c}{L}\right)\right], \end{aligned} \tag{10}$$

where $c = \frac{\pi\sigma^2}{knq_m G}$, $E(y)$ is the exponential integral, and the second equality is obtained by a change of variable to $y = L/z$. If we assume that the gradient and critical radius of the nucleus is such that nucleation only occurs at one temperature, T_c, the rate depends only on the first term of Eq. (10). To see how the overall growth rate V_g and the groove depth $D = L\cos\Theta$ are related, we plot $V_g \sin\Theta$ as a function of the groove depth in Fig. 6 for both cases described by Eq. (10). It is seen that the undercooling and hence nucleation rate at constant gradient must increase with groove depth and this will drive an increase in the overall growth rate. A principal influence of the spatial variation in the nucleation temperature is the more rapid rise in growth rate with groove depth.

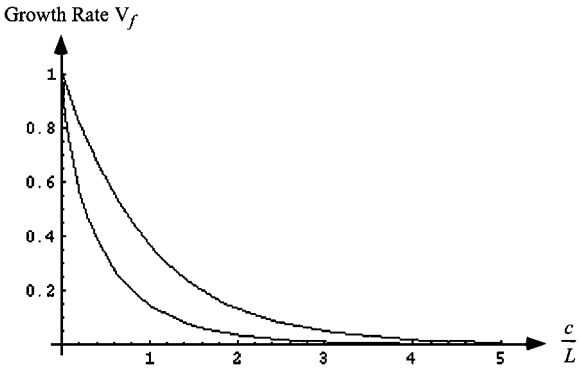

Figure 6. The growth rate $V_g \sin\Theta$ as a function of the groove depth for both cases described by Eq. (9). The upper curve assumes that nucleation occurs only at the cleft of the groove, hence is a pure exponential. The lower curve allows for the extension of nucleation probability over a finite distance above the cleft. Note the more rapid rise in growth rate with groove depth in the case where the spatial variation in the nucleation temperature is considered. Adapted from [73].

The rate of advance of the bulk interface at T_m is governed by the gradients in the ice and water, which control the dissipation of latent heat from the boundary. The net heat flux balance per unit area across the interface is therefore given by a Stefan condition

$$\rho q_m V_g = (k_i \nabla T_- - k_w \nabla T_+), \tag{11}$$

where ρ is the density of ice, and k_i and k_w are the thermal conductivities of ice and water, respectively. The depth D of the groove can be related to the temperature gradient and the speed of the interface. Since the temperature at the cleft $T_c = T_m - GL$, we can express the supercooling in terms of the speed by the modified Stefan condition:

$$T_m - T_c = \frac{D}{k_i}(\rho q_m V_g + k_w \nabla T_+). \tag{12}$$

Combining these expressions allows us to relate the overall motion to the depth of the groove under in

two cases. In the first, the spatial dependence of the nucleation probability is considered and in the second, nucleation occurs at one temperature. In the latter case we find

$$V_g = \frac{Ah}{\sin\Theta}\exp\left(-\frac{C}{DV_g}\right), \tag{13}$$

showing that at finite speed D depends on V_g transcendentally, where $C = cGk_i/\rho q_m$. This result obtains using the experimental observation that $\rho q_m V_g \gg k_w \nabla T_+$. We can obtain a simple approximation by taking the logarithm of Eq. (10): since $\ell n V_g$ is slowly varying, we can write

$$DV_g \approx \text{constant}, \tag{14}$$

displaying the inverse proportionality between the groove depth and the overall motion of the bulk interface.

3. Groove Dynamics at Moderate Freezing Rates. The dynamics discussed above assume that each layer is completed before the next layer is nucleated, so that the orientation of the groove surface is parallel to the principal crystal plane. When such a slow growth condition no longer holds, the geometry will change because it becomes possible that the nucleation time is shorter than the time for a layer to be completed, and hence new layers are successively nucleated on top of uncompleted layers; a multiple step regime is thus realized.

The groove angle Θ, is given by the ratio of normal and parallel speeds of the interface. Equations (7) and (8) relate the nucleation time, temperature and hence normal speed. However, there are no such simple relationships that allow us to relate the speed of growth of a layer *along* a facet to τ_p. Consider for example a step edge momentarily at an intermediate position z along the facet. The edge moves at a speed, V_p, controlled by the dissipation of latent heat into the adjacent ice and water, which is proportional to the local temperature difference $T_m - T(z)$, and hence the step slows down as it approaches the bulk boundary at T_m. This consideration leads immediately to a surface orientation that varies along the depth of the groove, deviating from the slow growth case as

$$\Delta\Theta(z) = \tan^{-1}\left[\frac{V_f}{V_p(z)}\right]. \tag{15}$$

The surface thereby develops a rounded profile, increasingly rounded near the top of the groove. The problem of moderate growth displays unique aspects of the role of molecular kinetics in a class of "Stefan problems" which classically deal with nonsteady phase boundary motion limited by transient thermal fields [45, 78]. We find here both thermal dissipation and molecular considerations to be important in determining the interfacial geometry.

4. Experimental Observations. Dynamical experiments on faceted grain boundaries were first performed in a radial, two-dimensional geometry by Wilen and Dash [72]. Subsequently, a vertically oriented Hele-Shaw type cell was constructed using a pair of transparent 75 mm long by 25 mm wide by 1 mm thick single crystal sapphire windows that are separated by a 0.76 mm thick epoxy-fiberglass composite frame of slightly longer dimension [73]. The dimensions of the actual cell volume were 70 mm $\times$ 20 mm $\times$ 0.76 mm.

Solidification runs were recorded on video tape from which detailed analyses could be performed. The progress was typically as follows. The initiation of freezing was followed by rapid growth of a thin film of ice on the lower region of the cooled window. The ice developed needle-like structure and grew as feathery dendrites, and then evolved to a more oriented structure, with a fairly smooth ice-water interface oriented normal to the direction of advance, and grain boundaries parallel to the temperature gradient. The majority of the grooves at the intersection of two grains and the water interface were of the normal variety described by Eq. (6). However there were usually one or more large faceted grooves. Typical grooves were appreciably asymmetric, with angles $30^\circ < \Theta < 45^\circ$. During solidification the grooves usually translated with constant shape and orientation along the direction of the temperature gradient. The trajectory is recorded as a grain boundary that was revealed using polarimetry. Occasionally short jogs in the trajectory would occur, but the track usually continued close to the gradient direction for the entire length of the cell. The size of the grooves varied with freezing speed and gradients; the largest being nearly 3 mm deep.

IV. Conclusion

A complete description of growing crystals is challenging and active research area, requiring methodology that extends into the domain of nonequilibrium

statistical mechanics, thermodynamics, and transport theory. Many of the results we find for ice, are foundational and hence possess consequences in a host of other areas. As a "low temperature ceramic" ice has a number of advantages, the principal ones being its transparency, convenient temperature range, and the fact that it exhibits most of the fundamental crystal growth behavior of interest in other materials. Its central role in a variety of natural phenomena, for example in glaciers, frost figures, frozen lakes, and sea ice, offer yet another compelling reason to use ice as a model material.

The problems presented to us by the dynamics of ice crystal growth continue to test our best efforts and pose challenges whose solutions hold promise for fields well beyond the material that stimulated them.

Acknowledgments

I am particularly indebted to J.W. Cahn, J.G. Dash, H. Dosch, M. Elbaum, S.C. Fain, J.W.M. Frenken, Y. Furukawa, H.E. Huppert, H. Jónsson, M. Maruyama, J.F. Nye, M. Schick, V. Tsemekhman, N. Untersteiner, L. Wilen, M.G. Worster, and E. Yokoyama for conversations and collaborations on topics directly and indirectly related to this research. I thank V. Tsemekhman for providing comments on the manuscript and E. Rabkin for inviting me to write it. This work has been supported by NSF Grants INT97-25945, CHE99-80125, OPP95-23513, and ONR Grant N00014-94-1-0120.

Note

1. The free energy change of the two-dimensional nucleus/source system of i_T total molecules with a nucleus of i molecules is $\Delta G = \Delta G_i - T\Delta S_i$, where ΔG_i is the free energy of formation of the nucleus and ΔS_i is the configurational entropy associated with the reorganization of i molecules from the parent phase to the crystal. Because $i_T \gg i$ we can approximate $\Delta G = \Delta G_i$.

References

1. F.C. Frank, J. Glaciol. **13**, 535 (1974).
2. M. Faraday, Proc. Roy. Soc. **10**, 440 (1860).
3. U. Nakaya, *Snow Crystals* (Harvard Univ. Press, Cambridge, MA, 1954).
4. Y. Furukawa, Chemie in unserer Zeit. **31**, 58 (1997).
5. G. Wulff, Z. Krist. **34**, 449 (1901).
6. S. Balibar, F. Graner, and E. Rolley, Prog. Cryst. Growth & Charact. Mats. **26**, 51 (1993).
7. S.G Lipson and E. Polturak, Prog. Low. Temp. Phys. **11**, 128 (1987).
8. J.D. Weeks and G.H. Gilmer, Adv. Chem. Phys. **40**, 157 (1979).
9. C. Herring, Phys. Rev. **82**, 87 (1951).
10. J.W. Cahn and W.C. Carter, Metall. and Mat. Trans. **27A**, 1431 (1996).
11. J.C. Heyraud and J.J. Mètois, Surf. Sci. **177**, 213 (1986).
12. Y. Furukawa and S. Kohata, J. Cryst. Growth **129**, 571 (1993).
13. K. Koo, R. Anath, and W.N. Gill, Phys. Rev. A **44**, 3782 (1991).
14. P. Nozières, in [80].
15. J.W. Cahn, Acta Metall. **8**, 534 (1960).
16. M. den Nijs, J. Phys. A **30**, 397 (1997).
17. M. Elbaum, Phys. Rev. Lett. **67**, 2982 (1991).
18. M. Maruyama, Y. Kishimoto, and T. Sawada, J. Cryst. Growth **172**, 521 (1997).
19. D. Nenow and A. Trayanov, Surf. Sci. **213**, 488 (1989).
20. H. Löwen, Phys. Rep. **237**, 249 (1994).
21. J.W.M. Frenken and H.M. van Pinxteren, Surf. Sci. **307–309** (B), 728 (1994).
22. J.G. Dash, H.-Y. Fu, and J.S. Wettlaufer, Rep. Prog. Phys. **58**, 115 (1995).
23. D.W. Oxtoby, in *Ice Physics and the Natural Environment*, edited by J.S. Wettlaufer, J.G. Dash, and N. Untersteiner NATO ASI Vol. 56, Series I (Springer-Verlag, Heidelberg, 1999), pp. 23–38.
24. J.S. Wettlaufer, M.G. Worster, L.A. Wilen, and J.G. Dash, Phys. Rev. Lett. **76**, 3602 (1996).
25. D.-M. Zhu and J.G. Dash, Phys. Rev. Lett. **57**, 2959 (1986).
26. D.B. Pengra, D.-M. Zhu, and J.G. Dash, Surf. Sci. **245**, 125 (1991).
27. D. Beaglehole and P. Wilson, J. Phys. Chem. **98**, 8096 (1994).
28. R.R. Netz and D. Andelman, Phys. Rev. E. **55**, 687 (1997).
29. J.S. Wettlaufer, Phys. Rev. Lett. **82**, 2516 (1999).
30. J.G. Dash, B.L. Mason, and J.S. Wettlaufer, J. Geophys. Res. in press (2001).
31. I. Golecki and C. Jaccard, Phys. Lett. A **63**, 374 (1977).
32. D. Beaglehole and D. Nason, Surf. Sci. **96**, 357 (1980).
33. Y. Furukawa, M. Yamamoto, and T. Kuroda, J. Cryst. Growth **82**, 665 (1987).
34. M. Elbaum, S.G. Lipson, and J.G. Dash, J. Cryst. Growth **129**, 491 (1993).
35. A. Kouchi, Y. Furukawa, and T. Kuroda, J. Physique Coll. **48**, 675 (1987).
36. H. Dosch, A. Lied, and J.H. Bilgram, Surf. Sci. **327**, 145 (1995).
37. X. Wei, P. Miranda, and Y.R. Shen, Phys. Rev. Lett. **86**, 1554 (2001).
38. J.S. Wettlaufer, Phil. Trans. Roy. Soc. A **357**, 3403 (1999).
39. J.S. Wettlaufer and J.G. Dash, Sci. American **281**, 50 (2000).
40. T. Kuroda and R. Lacmann, J. Cryst. Growth **56**, 189 (1982).
41. T. Sei and T. Gonda, J. Cryst. Growth **94**, 697 (1989).
42. H. Nada and Y. Furukawa, Surf. Sci. **446**, 1 (2000).
43. J.S. Kirkaldy, Rep. Prog. Phys. **55**, 723 (1992).
44. M.C. Cross and P.C. Hohenberg, Rev. Mod. Phys. **65**, 851 (1993).
45. M.G. Worster, in *Perspectives in Fluid Dynamics—a Collective Introduction to Current Research*, edited by G.K. Batchelor, H.K. Moffatt, and M.G. Worster (Cambridge Univ. Press, Cambridge, MA, 2000), pp. 393–446.
46. Y. Carmi, S.G. Lipson, and E. Polturak, Phys. Rev. B **36**, 1894 (1987).
47. J.W. Cahn and J.E. Taylor, Acta Metall. **42**, 1045 (1994).

48. F.C. Frank, in *Growth and Perfection of Crystals*, edited by R.H. Doremus, B.W. Roberts, and D. Turnbull (Wiley, New York, 1958), pp. 411–419.
49. A.A. Chernov, Sov. Phys.-Crystallog. **7**, 728 (1963).
50. J. Villain, Nature **350**, 273 (1991).
51. M. Maruyama, N. Kuribayashi, K. Kawabata, and J.S. Wettlaufer, Phys. Rev. Lett **85**, 2545 (2000).
52. J. Taylor, J.W. Cahn, and C.A. Handwerker, Acta Met. **40**, 1443 (1992).
53. M. Elbaum and J.S. Wettlaufer, Phys. Rev. E **48**, 3180 (1993).
54. J.S. Wettlaufer, M. Jackson, and M. Elbaum, J. Phys. A **27**, 5957 (1994).
55. H. Müller-Krumbhaar, T.W. Burkhardt, and D.M. Kroll, J. Cryst. Growth **38**, 13 (1977).
56. M. Uwaha, J. Cryst. Growth **80**, 84 (1987).
57. E. Yokoyama and R.F. Sekerka, J. Cryst. Growth **125**, 389 (1992).
58. E. Yokoyama, R.F. Sekerka, and Y. Furukawa, J. Phys. Chem. B **104**, 65 (2000).
59. J. Flesselles, M.O. Magnasco, and A.J. Libchaber, Phys. Rev. Lett. **67**, 2489 (1991).
60. B. Berge, L. Faucheux, K. Schwab, and A.J. Libchaber, Nature **350**, 322 (1991).
61. S. Angenent and M.E. Gurtin, Arch. Ration. Mech. Anal. **104**, 323 (1989).
62. J.S. Langer, in *Chance and Matter*, edited by J. Souletie, J. Vannimenus, and R. Stora (North Holland, New York, 1987), pp. 629–711.
63. C.E. Weir, G.J. Piermarini, and S. Block, J. Chem. Phys. **50**, 2089 (1969).
64. T. Yagi, J. Japan. Assoc. Cryst. Growth **8**, 166 (1981).
65. V. Tsemekhman and J.S. Wettlaufer (to be published).
66. F. Bolling and W.A. Tiller, J. Appl. Phys. **31**, 1345 (1960).
67. G.E. Nash and M.E. Glicksman, Phil. Mag. **24**, 577 (1971).
68. R.J. Schaefer, M.E. Glicksman, and J.D. Ayers, Phil. Mag. **32**, 725 (1977).
69. S.C. Hardy, Phil. Mag. **35**, 471 (1977).
70. P.W. Voorhees, S.R. Coriell, G.B. McFadden, and R.F. Sekerka, J. Cryst. Growth **67**, 425 (1984).
71. L.A. Wilen and J.G. Dash, Science **270**, 1184 (1995).
72. J.G. Dash, V.A. Hodgkin, and J.S. Wettlaufer, J. Stat. Phys. **95**, 1311 (1999).
73. W.K. Burton, N. Cabrera, and F.C. Frank, Phil. Trans. Roy. Soc. A. **243**, 299 (1951).
74. W.B. Hillig, in *Growth and Perfection of Crystals*, edited by R. H. Doremus, B.W. Roberts, and D. Turnbull (Wiley, New York, 1958), pp. 350–360.
75. D. Turnbull, in *Solid State Physics*, edited by F. Seitz and D. Turnbull (Academic Press, New York, 1956), Vol. 7, pp. 226–308.
76. P.R. Pennington, S.F. Ravitz, and G. Abbaschian, Acta Metall. **18**, 943 (1970).
77. J.S. Wettlaufer, *Festschrift 150 Jahre Institut für Met. und Geophysik, Univ. Wien* (Styria Verlag, Graz, 2001).
78. C. Godreche, *Solids far from Equilibrium* (Cambridge Univ. Press, Cambridge, MA, 1991).